Prediction of Charge-Induced Molecular Alignment of Biomolecules Dissolved in Dilute Liquid-Crystalline Phases

Markus Zweckstetter,* Gerhard Hummer,† and Ad Bax†
*Max Planck Institute for Biophysical Chemistry, Am Fassberg, Göttingen, Germany; and †Laboratory of Chemical Physics, National Institute of Diabetes and Digestive and Kidney Diseases, National Institutes of Health, Bethesda, Maryland USA

ABSTRACT Alignment of macromolecules in nearly neutral aqueous lyotropic liquid-crystalline media such as bicelles, commonly used in macromolecular NMR studies, can be predicted accurately by a steric obstruction model (Zweckstetter and Bax, 2000). A simple extension of this model is described that results in improved predictions for both the alignment orientation and magnitude of protein and DNA solutes in charged nematic media, such as the widely used medium of filamentous phage Pf1. The extended model approximates the electrostatic interaction between a solute and an ordered phage particle as that between the solute's surface charges and the electric field of the phage. The model is evaluated for four different proteins and a DNA oligomer. Results indicate that alignment in charged nematic media is a function not only of the solute's shape, but also of its electric multipole moments of net charge, dipole, and quadrupole. The relative importance of these terms varies greatly from one macromolecule to another, and evaluation of the experimental data indicates that these terms scale differently with ionic strength. For several of the proteins, the calculated alignment is sensitive to the precise position of the charged groups on the protein surface. This suggests that NMR alignment measurements can potentially be used to probe protein electrostatics. Inclusion of electrostatic interactions in addition to steric effects makes the extended model applicable to all liquid crystals used in biological NMR to date.

INTRODUCTION

Measurement of global orientational constraints, such as residual dipolar couplings (RDCs), offers many new opportunities in NMR studies of macromolecules in solution, ranging from structure validation and rapid structure determination to the study of dynamics (Clore et al., 1998; Cornilescu et al., 1998; Delaglio et al., 2000; Hansen et al., 1998; Hus et al., 2001; Meiler et al., 2001; Tjandra et al., 1997; Tolman, 2002; Tolman et al., 1995). This technology relies on weak alignment of the macromolecule in solution, usually accomplished by means of a dilute liquid-crystalline medium (Barrientos et al., 2000, 2001; Clore et al., 1998; Fleming et al., 2000; Hansen et al., 1998; Prestegard and Kishore, 2001; Prosser et al., 1998; Ruckert and Otting, 2000; Tjandra and Bax, 1997).

Previously, we and others have shown that alignment in nematic phases of neutral (undoped) bicelles is dominated by steric effects, and that the molecular alignment tensor can be predicted accurately on the basis of the molecule's three-dimensional shape (Almond and Axelsen, 2002; Fernandes et al., 2001; Zweckstetter and Bax, 2000). Predicted alignment tensors for a given structure have been used for the differentiation of monomeric and homodimeric states (Zweckstetter and Bax, 2000), conformational analysis of dynamic systems such as oligosaccharides (Azurmendi and Bush, 2002), refinement of nucleic acid structures (Warren and Moore, 2001), determination of the relative orientation of protein domains (Bewley and Clore, 2000), and validation of structures of protein complexes (Bewley, 2001). The ability to predict dipolar couplings for a given protein structure also provides unique opportunities when attempting to classify protein fold families on the basis of unassigned NMR data, potentially increasing data throughput in structural genomics (Valafar and Prestegard, 2003).

Solute alignment can be altered considerably by adding net charge to bicelles (Ramirez and Bax, 1998). As a direct consequence, the prediction of macromolecular alignment based on steric obstruction fails completely for highly charged liquid-crystalline media (Zweckstetter and Bax, 2000) such as the popular nematic phases of phage particles *fd* and Pf1 (Clore et al., 1998; Hansen et al., 1998).

Analysis of solute alignment observed in apolar organic liquid-crystalline media shows that steric interactions frequently dominate, but electrostatic forces can be important (Dingemans et al., 2003; Terzis et al., 1996). There is still much debate as to which electrostatic interactions are most important. Some studies indicate that in apolar media it is primarily the electric quadrupole moment of the solute that dominates its alignment (Syvitski and Burnell, 1997, 2000). Other studies argue that the dipole moment plays a major role (Photinos et al., 1992; Photinos and Samulski, 1993). In aqueous solution, full calculation of electrostatic forces between charged macromolecules is a very complex and computationally demanding problem (Davis and McCammon, 1990; Emsley et al., 1991; Honig et al., 1993; Vroege and Lekkerkerker, 1992; Warshel and Aqvist, 1991).

Here, we demonstrate that for aqueous lyotropic liquid-crystalline media, such as that of filamentous phage, a highly

Submitted October 10, 2003, and accepted for publication February 9, 2004.

Address reprint requests to Dr. Markus Zweckstetter, Max Planck Institute for Biophysical Chemistry, Am Fassberg 11, D-37077 Göttingen, Germany. Tel.: 49-551-201-2220; E-mail: mzwecks@gwdg.de.

0006-3495/04/06/3444/17 $2.00

doi: 10.1529/biophysj.103.035790

oversimplified model, which approximates the electrostatic interaction between a solute and an ordered phage particle as that between the solute surface charges and the electric field of the phage, predicts both the magnitude and orientation of the solute's alignment tensor with reasonable accuracy. Our results demonstrate that in charged liquid-crystalline media electrostatic and steric interactions are the two major contributors to solute ordering. In contrast to the case of steric ordering, we find that depending on the system studied the predicted alignment can be quite sensitive to structural details of the model, in particular the precise location of charged groups on the surface of a protein.

A very recent and independent study by Ferrarini proposes a similar method to predict alignment in charged nematic media and compares experimental dipolar couplings of the first Igg-binding domain of protein G (GB1) with couplings predicted on the basis of its third Igg-binding domain (GB3) (Ferrarini, 2003). The program we describe here and make available predicts rather different alignment for the GB1 and GB3, resulting from their different surface charge distributions, but shows reasonable agreement with experimental data over a wide range of ionic strength. The program also permits evaluation of the contributions from net charge, dipole, and quadrupole moments to ordering, and application to four different proteins and a DNA dodecamer indicates that the relative importance of these terms varies strongly with the system studied.

MATERIALS AND METHODS

Sample preparation

Dipolar coupling data were collected for four small proteins dissolved in dilute suspensions of Pf1 bacteriophage: ubiquitin, the RecA-inactivating protein DinI, and the first and third Igg-binding domains of protein G, GB1 and GB3. Pf1 phage was purchased from ASLA (Riga, Latvia; http://www.asla-biotech.com/asla-phage.htm). $^{13}C/^{15}N/^{2}H$-enriched ubiquitin was prepared as described by Sass et al. (1999) and kindly provided to us by S. Grzesiek. ^{15}N-enriched RecA binding protein DinI and ^{15}N-enriched GB1 and GB3 were prepared as described previously (Gronenborn et al., 1991; Ramirez et al., 2000). NMR samples contained 1 mM ubiquitin, 0.3 mM DinI, 0.2 mM GB1, and 2 mM GB3 in 90% H_2O/10% D_2O, pH 7. Titration studies were also carried out for a selectively $^{13}C/^{15}N$-labeled dodecamer, d(CGCGAATTCGCG)$_2$ (Tjandra et al., 2000) with the uniformly ^{13}C-enriched nucleotides indicated by underlines.

NMR spectroscopy and processing

All NMR experiments were carried out at 25°C, in thin-wall Shigemi microcells (Shigemi, Allison Park, PA) on Bruker DRX600 (ubiquitin, DinI, GB1) and DRX800 (GB3, Dickerson dodecamer) spectrometers (Bruker, Billerica, MA) equipped with three-axis pulsed field-gradient $^{1}H/^{15}N/^{13}C$ probeheads. Residual ^{15}N-^{1}H dipolar couplings in the four proteins were derived from in-phase/anti-phase (IPAP) [^{15}N, ^{1}H]-heteronuclear single quantum coherence (HSQC) experiments (Ottiger et al., 1998). One-bond sugar $^{1}D_{CH}$ RDCs in the Dickerson dodecamer were measured from F_1-coupled ^{1}H-^{13}C HSQC spectra. Spectra were processed and analyzed using NMRPipe/NMRDraw (Delaglio et al., 1995).

Determination of Pf1 concentration

Although reasonable quantitative estimates of the Pf1 concentration can be obtained from its ultraviolet absorbance at 270 nm, using an extinction coefficient of 2.25 cm^{-1} mg^{-1} ml, a more convenient way to characterize Pf1 concentration simply monitors the lock solvent quadrupole splitting, $Q_{cc}(^{2}H)$. As incomplete Pf1 ordering in the paranematic phase scales $Q_{cc}(^{2}H)$ by the same factor as the observed dipolar splittings for the solute (Zweckstetter and Bax, 2001), this makes it straightforward to reference all results reported in this study to a single Pf1 concentration, which was chosen to be 17 mg/ml, corresponding to a $Q_{cc}(^{2}H)$ splitting of 15 Hz.

Salt titrations

The change in alignment strength and orientation was investigated for a variety of ionic strengths. Titrations were started at very low ionic strength and the ionic strength was continuously increased by addition of 1 M (low ionic strength) or 4 M (high ionic strength) NaCl solutions. In total, ^{15}N-^{1}H dipolar couplings were measured in DinI at NaCl concentrations of 30, 50, 110, 210, 315, 400, and 500 mM; in ubiquitin at 20, 50, 105, 240, 340, and 450 mM NaCl; in GB3 at 10, 20, 54, 105, 210, 360, and 500 mM NaCl; and in GB1 at 10, 20, 53, 105, 206, 300, 400, and 500 mM NaCl. To overcome problems associated with very strong ordering at low ionic strength, dipolar coupling measurements in ubiquitin, DinI, and GB3 needed to be performed at dilute Pf1 concentrations.

For DinI and GB3, starting concentrations of 12 mg/ml (quadrupole splitting of the solvent ^{2}H resonance $Q_{cc}(^{2}H) = 10.7$ Hz) and 9.3 mg/ml Pf1 ($Q_{cc}(^{2}H) = 8.2$ Hz), respectively, were used (Zweckstetter and Bax, 2001). Ubiquitin aligns very strongly and the starting Pf1 concentration had to be reduced to ~4 mg/ml, with the result that the titration is already started in the paranematic region. To evaluate ordering in the fully liquid-crystalline state, ubiquitin dipolar couplings were also measured using 20.5 mg/ml Pf1 and 240 mM NaCl.

For titration of the Dickerson dodecamer, the sample was initially washed multiple times with an 8 mM NaCl buffer (pH 6.8). RDCs were measured at five different salt concentrations: 8, 50, 100, 210, and 300 mM NaCl. The starting concentration of Pf1 was 26.2 mg/ml ($Q_{cc}(^{2}H) = 23.2$ Hz). During the titration series, this quadrupole splitting decreased to 20 Hz, but again, all data have been rescaled to 17 mg/ml Pf1 concentration. Errors in $^{1}D_{CH}$ measurements are below 1 Hz and therefore have negligible influence on the error in alignment tensor, which is dominated by errors in the atomic coordinates.

Analysis of experimental residual dipolar couplings

Alignment tensors in liquid-crystalline or paranematic Pf1 were obtained by fitting one-bond RDCs to high-resolution NMR (for DinI, ubiquitin, and DNA: mean of 1GHH, Ramirez et al., 2000; 1D3Z, Cornilescu et al., 1998; and 1DUF, Tjandra et al., 2000, respectively) or crystal structures (for GB3: residues 6–61 of 1IGD, Derrick and Wigley, 1994; for GB1: 1PGA, Gallagher et al., 1994), using singular value decomposition (SVD) (Losonczi et al., 1998) as implemented in the program PALES (M. Zweckstetter, unpublished). For x-ray structures hydrogens were added using the program MOLMOL (Koradi et al., 1996). Errors in these alignment tensors are mainly influenced by uncertainties in the reference structures. These errors were estimated using a Monte Carlo structural noise method recently introduced (Zweckstetter and Bax, 2002). DinI aligns very strongly at 30 and 50 mM NaCl, 12 mg/ml Pf1, and only nine ^{15}N-^{1}H RDCs could be measured. To avoid large errors in ordering strength introduced by structural noise during SVD, the alignment magnitude at these salt concentrations was determined from its value at 100 mM using the scaling of RDCs when going from 100 to 30 or 50 mM NaCl (neglecting any change in alignment tensor orientation).

Implementation of charge/shape prediction

The charge/shape prediction has been implemented into the dipolar coupling analysis software PALES using the C programming language. To make argument lists more concise, default parameters are used in the absence of additional command-line arguments. Thus, the minimal input to the program consists of a file name containing the structure coordinates, the pH of interest, the concentration of the liquid-crystalline medium, and the ionic strength. In addition, electrostatic potentials can be supplied, user defined charges can be read, the order parameter of the liquid crystal and its average surface charge can be adjusted, and experimental dipolar couplings can be compared to those simulated. A charge/shape simulation using the full-charge model for a protein of 80 residues can be performed in about 1 min on a single processor SGI origin (270 MHz) workstation (Silicon Graphics, Houston, TX). Use of a multipole expansion speeds up the calculation, particularly for larger proteins as only a total of ten charges is taken into account.

Calculation of electrostatic interactions

In our simplified model, proteins and nucleic acids, as charged polymers, are represented by the charges of their ionizable residues. The current studies were performed at pH 7. Therefore, all ionizable residues, except for histidine, are assumed to be fully charged (charge of 1.0 e for Arg and Lys, charge of −1.0 e for Glu and Asp). The N- and C-termini also carry a charge of 1.0 e and −1.0 e, respectively. The protonation state of His is calculated by the program using the Henderson-Hasselbach equation, assuming a reference pKa of 6.3 (charge of 0.33 e at pH 7; Antosiewicz et al., 1994). Charges are distributed evenly over the heavy atoms involved (e.g., both N^{η} atoms for Arg, but only N^{ξ} for Lys). Considering more detailed charge models for histidines or other side-chain charges (such as deviations from default pK values) did not consistently improve the quality of our charge/shape prediction, but introduces additional simulation parameters and was therefore not used. Similarly, use of partial charges for the remaining atoms, as defined in CHARMM TOPH19 parameter set, is found to have only a small effect (compared to other factors such as the quality of the reference structure) on predicted alignment tensors. Placing effective charges only at the positions of ionizable residues reduces the total number of charges needed to calculate the electrostatic interactions, and therefore speeds up the computation significantly. For example, for DinI, only 46 instead of 502 charges needed to be used.

Obstruction effects were evaluated using only surface accessible atoms. Surface-accessible atoms were determined using a double cubic lattice method (Eisenhaber and Argos, 1993). For calculation of surface accessibility atom radii were taken from Eisenberg and McLachlan (1986). The solvent radius was set equal to 1.4 Å. To evaluate steric clash between the solute and the liquid crystal particle, radii of solute atoms were set to zero. This allows the solute to access all values of the electrostatic potentials, even the very high values close to the surface of the liquid crystal particle.

For bacteriophage Pf1 a cylinder radius of 3.35 nm, a density of 1.46 g/cm^3, a surface charge density of −0.475 e/nm^2, and a liquid crystal order parameter of 0.9 was used (Zimmermann et al., 1986). The static dielectric constant of water was set to 78.29. Electrostatic potentials for Pf1 bacteriophage were once calculated outside of PALES, and stored as values on a grid with a distance spacing of 0.1 Å between grid points. These potentials are read into PALES and a linear weighting scheme is used to interpolate between grid points. In case of planar liquid crystal particles electrostatic potentials are calculated within PALES from the analytical solution of the nonlinear Poisson-Boltzmann (PB) equation. To reduce calculation times, especially in case of very low liquid crystal concentrations, electrostatic interactions were evaluated until the potential had dropped to 10^{-5} (k_BT)/e. At and below potentials of 10^{-5} (k_BT)/e the Boltzmann factor p_B is negligible and introduction of this cut-off has no influence on simulated alignment tensors.

We tested the convergence of the results with respect to the spacing of the one-dimensional grid along which the geometric center of the molecule is moved. Increasing the spacing between grid points from 0.2 to 0.5 and to 2.0 Å changes the orientation of the alignment tensor predicted for DinI at 0.20 M NaCl by <3°. Similarly, sampling 362 instead of 122 orientations on the unit sphere and simultaneously increasing the sampling in the third dimension from 18 to 36, i.e., sampling a total of 13,032 instead of 2196 orientations, changes the orientation of the alignment tensor predicted for DinI at 0.20 M NaCl by <2°. Therefore, for all results presented in this study, only 2196 orientations were used.

Analysis of charge/shape-predicted alignment tensors

The accuracy of the magnitude of predicted alignment tensors is assessed using a generalized alignment tensor magnitude,

$$G_{\mathrm{Mag}} = (2D_{\mathrm{a}}/D_{\mathrm{max}}^{\mathrm{PQ}})[\pi(4 + 3R^2)/5]^{1/2}, \qquad (1)$$

where $D_{\mathrm{max}}^{\mathrm{PQ}} = -\mu_0(h/2\pi)\gamma_{\mathrm{P}}\gamma_{\mathrm{Q}}/(4\pi^2 r_{\mathrm{PQ}}^3)$, with μ_0 the permittivity of vacuum, h Planck's constant, γ the magnetogyric ratio, and r_{PQ} the PQ internuclear distance. In addition, D_{a} values are used, as visualization of the meaning of ordering parameters is frequently carried out using diagonalized alignment tensors. To evaluate to which degree the orientation of experimental alignment tensors can be predicted, we compare predicted RDCs with experimental ones using Pearson's linear correlation coefficient R_{P}. This directly addresses the question of how well experimental dipolar couplings can be predicted using our simple model, and avoids errors in experimental alignment tensor orientations introduced by SVD. Finally, the change in experimental alignment tensor orientations with increasing ionic strength is monitored by comparison of RDCs observed at low salt with those measured at later stages of the titration.

Software availability

The program used in the present study, which includes all features of the earlier steric prediction, too, is available upon request from M.Z. (mzwecks@gwdg.de) for SGI and Linux machines.

RESULTS

Computational approach

Our new method is an extension of the steric obstruction algorithm, described previously (Zweckstetter and Bax, 2000). In the original method, the nematogen is approximated by an infinite wall (bicelles) or infinite cylinder (Pf1 bacteriophage), oriented parallel to the magnetic field (z axis). The center of gravity of the solute is moved on a one-dimensional grid, with a spacing between grid points of 0.2 Å, away from the surface of the liquid crystal model. At each step, a set of 2196 different molecular orientations is sampled. These 2196 orientations are obtained in a two-step procedure. First, the z axis of the molecule samples 122 points on a unit sphere that were determined by a double cubic lattice method (Eisenhaber et al., 1995). This provides a highly uniform sampling of the sphere. The remaining deviation from a completely uniform sampling corresponds to a residual alignment that corresponds to a generalized magnitude, G_{Mag}, of the alignment tensor (Eq. 1) (Sass et al.,

1999) that is smaller than 10^{-7}. With typical experimental alignment strength of $G_{Mag} \sim 10^{-3}$ (see Table 1) this introduces negligible errors into the calculations. In a second step, the molecule is rotated around the z axis in steps of 20°.

For each orientation the program evaluates whether the solute sterically clashes with the nematogen, i.e., if any of the solute atoms has a coordinate within the wall or cylinder model. If this is not the case an alignment matrix **A** is calculated

$$A_{ij} = 1/2(3\cos\theta_i \cos\theta_j - \delta_{ij})(i,j = x,y,z), \qquad (2)$$

where θ_i indicates the angle between the i^{th} molecular axis and the z axis (magnetic field direction) and δ_{ij} the Kronecker delta. In the original, steric model the overall molecular alignment tensor, $\mathbf{A}^{mol}$, is simply the linear average over all nonexcluded **A** matrices (Eq. 2). In the electrostatic extension of this model, each nonexcluded **A** matrix is weighted according to its Boltzmann probability, after calculating the corresponding electrostatic potential of the solute (see below). Using periodic boundary conditions, sampling is restricted to distances r between the solute center of gravity and the center of the bilayer or cylinder for which $r < d/(2V_f)$ (wall model), or $r < d/(4V_f)^{1/2}$ (cylinder), where d is either the wall thickness (40 Å for bicelles) or the cylinder diameter (67 Å for Pf1), and V_f is the nematogen volume fraction. The imperfect alignment of liquid crystals is taken into account by multiplication of $\mathbf{A}^{mol}$ with the order parameter of the liquid crystal.

TABLE 1 Experimental, SVD-derived alignment tensor values and correlation between experimental and structure-predicted couplings as a function of ionic strength

NaCl (mM)	$Q_{cc}(^2H)$* (Hz)	G_{Mag} ($\times 10^{-4}$)	D_a(NH) (Hz)	D_r/D_a	α(°)	β(°)	γ(°)	R_P
			GB3					
10	8.25	33.7	22.9	0.10	20	90	123	0.98
20	7.79	29.7	20.2	0.10	20	89	124	0.98
54	6.95	20.4	13.8	0.11	13	89	125	0.98
105	6.25	15.0	10.1	0.14	9	89	126	0.98
210	5.00	7.0	4.7	0.23	5	89	129	0.98
360	3.90	3.7	2.5	0.32	1	90	132	0.98
500	3.10	2.4	1.5	0.39	178	92	135	0.98
			GB1					
10	24.67	13.2	−7.9	0.64	168	1233	161	0.98
20	24.06	12.4	−7.3	0.65	171	123	162	0.98
53	23.73	12.0	−7.1	0.66	177	124	163	0.97
105	23.44	10.7	−6.3	0.66	182	130	165	0.97
206	22.10	8.9	5.3	0.67	132	103	67	0.97
300	21.00	7.7	4.8	0.54	125	110	60	0.96
400	19.50	7.0	4.2	0.58	115	113	57	0.96
500	18.45	6.5	4.0	0.54	105	118	47	0.97
			Ubiquitin					
20	0.70	8.1	5.0	0.53	137	56	36	0.98
50	0.65	4.0	2.4	0.58	131	47	38	0.97
105	0.61	2.6	1.6	0.55	130	47	40	0.96
240	0.60	1.1	−0.7	0.27	52	66	279	0.96
340	0.45	0.6	−0.4	0.23	82	63	280	0.91
450†	0.43	0.5	−0.3	0.49	86	62	295	0.72
			DinI					
110	9.53	37.3	25.3	0.11	88	130	146	0.99
210	8.34	21.1	14.2	0.14	68	131	148	0.99
315	7.30	13.2	8.8	0.21	63	133	151	0.99
400	6.10	8.6	5.7	0.30	63	134	153	0.99
500	5.34	6.2	4.0	0.42	72	134	156	0.94

The alignment tensor is characterized by the axial component D_a(NH), the rhombicity D_r/D_a and the three Euler angles α, β, and γ. The Euler angles are defined by three clockwise rotations around the z, y', and z'' axes and specify the orientation of the alignment tensor relative to the coordinate frame of the PDB structure.

*Value of the solvent ^{2}H quadrupole splitting, reflecting Pf1 concentration.

†Corresponding alignment tensor values have a significantly higher uncertainty resulting from the low degree of alignment and the correspondingly small experimental dipolar couplings.

Continuum electrostatic theory (Debye and Hueckel, 1923) is used for calculating the electrostatic interaction energy: the solute is embedded in a dielectric medium containing excess ions, in addition to the counterions neutralizing the solute and nematogen. The nonlinear PB equation is used to derive the electrostatic potential (Chapman, 1913; Gouy, 1910). Even within the simplifications of a continuum description, calculation of the electrostatic potential would require solving a full three-dimensional electrostatics problem for each distance and orientation of the solute with respect to the surface of the charged liquid crystal particle. Instead, we further simplify the problem by treating the solute as a particle in the external field of the liquid crystal. Moreover, we assume the nematogen to carry a uniform charge density instead of discrete surface charges. The nonlinear three-dimensional PB equation is then solved only once, in the absence of the solute, yielding an electrostatic potential $\varphi(\mathbf{r})$. The distance and orientation-dependent electrostatic free energy of the protein comprising partial charges q_i at positions $\mathbf{r}_i$ is then approximated by

$$\Delta G_{el}(\mathbf{r},\mathbf{\Omega}) = \textstyle\sum_i q_i \phi[\mathbf{r}_i(\mathbf{r},\mathbf{\Omega})]. \qquad (3)$$

The Boltzmann factor $p_B = exp[-\Delta G_{el}(\mathbf{r},\mathbf{\Omega})/k_B T]$ provides relative electrostatic weights when averaging the individual alignment tensors, derived for each orientation and distance (Eq. 3), to yield an overall solute alignment tensor

$$\mathbf{A}_{ij}^{mol} = \int \mathbf{A}_{ij} p_B(\mathbf{r},\mathbf{\Omega}) d\mathbf{r} d\Omega \Big/ \int p_B(\mathbf{r},\mathbf{\Omega}) d\mathbf{r} d\Omega. \qquad (4)$$

For a flat surface an analytical solution of the nonlinear PB equation exists (Chapman, 1913; Gouy, 1910). For uniformly charged cylinders (bacteriophage) the method of Stigter (1982a,b) is used assuming symmetric monovalent ions and vanishing potential at infinity. We also solved the PB equation with Neumann boundary conditions, i.e., zero normal derivative on an outer cylinder of radius r, to mimic the situation in a two-dimensional, hexagonally packed lattice of phages with neutral unit cells (Hummer et al.,

1998). This, however, does not lead to significant changes. For an outer radius of $r = 200$ Å and salt concentrations above 0.01 M, the differences between the two solutions are confined to the outer boundary region, where the potentials are already very weak (data not shown). This can be understood using charge neutralization arguments: If the Debye length $1/\kappa$ is much smaller than r, the phage is charge neutralized well before reaching the outer boundary. The two boundary conditions lead to substantially different results only if $1/\kappa$ is similar to r or larger.

Prediction of charge-induced molecular alignment

Experimental RDCs have been measured in four different proteins and a DNA oligomer d(CGCGAATTCGCG)$_2$, often referred to as the Dickerson dodecamer (Dickerson and Drew, 1981). For each molecule a high-resolution x-ray or NMR structure is available and experimental RDCs fit well to the structures when evaluated by SVD (Table 1; Fig. 1). These RDCs and structures were used to evaluate the validity of Eq. 4.

Fig. 2 compares experimental RDCs observed in the five macromolecules with values predicted on the basis of their three-dimensional shape. For the four proteins, ^{15}N-^{1}H dipolar couplings ($^{1}D_{NH}$) predicted on the basis of a purely steric mechanism correlate poorly with those experimentally observed, with correlation coefficients, R_P, of 0.77, 0.34, 0.07, and 0.19 for ubiquitin, DinI, GB3, and GB1, respectively (Fig. 2, *A–D*). Moreover, for ubiquitin, DinI, and GB3 the alignment strength is severely underestimated. For example for ubiquitin the shape-predicted dipolar couplings are fivefold smaller than what is observed experimentally. Note, however, that based on a purely steric mechanism such small RDCs are actually expected, as only 17 mg/ml of Pf1 (corresponding to a volume fraction of only 1.2%) are used, compared to routinely used concentrations of 3–6% v/v in case of bicelles. This already indicates that in highly charged liquid-crystalline media, such as bacteriophage Pf1, interactions other than obstruction are important for molecular ordering.

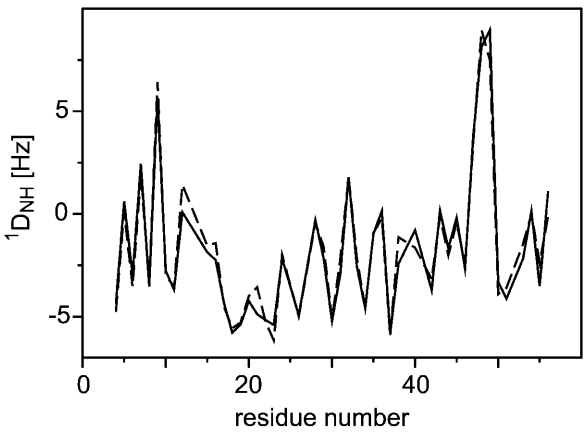

FIGURE 1 Experimental $^{1}D_{NH}$ values at 0.20 M NaCl (*solid line*) and $^{1}D_{NH}$ values best-fitted to the 1.1 Å crystal structure of GB3 (PDB code: 1IGD) (*dashed line*). The dipolar coupling quality factor Q (Ottiger and Bax, 1999) is 10%.

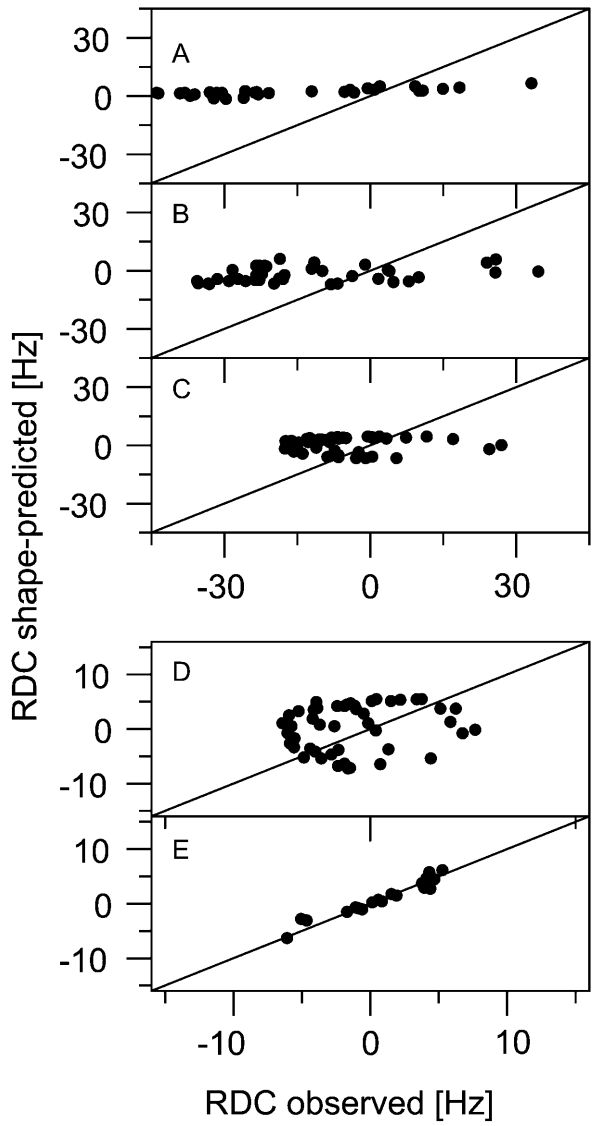

FIGURE 2 Comparison of experimental $^{1}D_{NH}$ values with values predicted on the basis of the molecules' three-dimensional shapes (not taking into account electrostatic effects) for ubiquitin (*A*), DinI (*B*), GB3 (*C*), GB1 (*D*), and the Dickerson dodecamer (*E*). Experimental values were obtained at 0.20 M NaCl, pH 7, 25°C, using Pf1 bacteriophage as alignment medium. Experimental and predicted $^{1}D_{NH}$ values were rescaled to 17 mg/ml Pf1. High-resolution NMR (PDB codes for DinI, ubiquitin, and DNA: 1GHH, 1D3Z, and 1DUF, respectively) or crystal structures (for GB3: residues 6–61 of 1IGD; for GB1: 1PGA) were used for shape prediction. Straight lines correspond to $y = x$.

The situation is different for the Dickerson dodecamer. Experimental RDCs fit very well to shape-predicted values (Fig. 2 *E*). As discussed below, this results from the DNA's negative charge properties. The electrostatic repulsion between the negatively charged Pf1 surface and the DNA

phosphate backbone charges does not significantly affect the preferred orientation of the Dickerson dodecamer in the dilute Pf1 suspension, i.e., its alignment tensor orientation. On the other hand, it may appear surprising that even the magnitude of the alignment tensor is predicted correctly by the steric model, despite the strong electrostatic repulsion. As discussed in more detail in the section ''Prediction of alignment using empirical correction factors'', this results from two compensating effects: positions close to the surface of Pf1, which would highly orient through steric means, are less populated by DNA molecules due to electrostatic repulsion, whereas positions where no steric clash between the Dickerson dodecamer and Pf1 occurs now contribute to the overall alignment due to electrostatic interaction. Thus, the alignment magnitude will depend on the relative weight of electrostatic and steric contributions to molecular ordering, and therefore on the specific shape and total net charge of the nucleic acid of interest. Therefore, unless these contributions are exactly balanced, shape-predicted alignment magnitudes for nucleic acids, dissolved in highly charged liquid-crystalline media, are not expected to agree with experimental values.

Does inclusion of electrostatic interactions, treated in the highly simplified manner described above, improve the prediction of residual dipolar couplings from a known three-dimensional structure? The answer to this question is obtained by inspection of Fig. 3. For all four proteins much improved agreement between predicted and observed RDCs is observed compared with the shape-predicted values of Fig. 2. For the 81-residue recA-binding protein DinI, experimental $^1D_{NH}$ values agree almost perfectly with those predicted on the basis of DinI's charge/shape model (Ramirez et al., 2000), with a Pearson's correlation coefficient $R_P = 0.96$ (Fig. 3 *B*). In addition, the alignment magnitude of $G_{Mag} = 3.2 \times 10^{-3}$ predicted at 17 mg/ml Pf1 is close to the experimental value of $G_{Mag} = 4.1 \times 10^{-3}$ (Table 1). With $R_P = 0.95$, the prediction quality for ubiquitin is comparable to that of DinI. The magnitude of ubiquitin's alignment is also much better predicted by the charge/shape model than by the pure shape model (compare Fig. 3 *A* with Fig. 2 *A*). For GB3 and GB1 the quality of the predictions is lower, with $R_P = 0.88$ and $R_P = 0.75$, respectively.

Similar results are obtained for salt concentrations from 0.02 to 0.50 M NaCl (Fig. 4). The RDCs predicted from the shape and side-chain charges of biomolecules correlate quite well with experimental values. Except for ubiquitin above 0.30 M NaCl, where experimental RDCs are less accurate (Table 1), correlation factors R_P are above 0.9 for ubiquitin, DinI and the Dickerson dodecamer. For GB3 and GB1 the quality of prediction is generally lower, with R_P values ranging from 0.69 to 0.94. The slight improvement when going to higher ionic strengths is due to the increased contribution from steric alignment for these two proteins (see discussion in the section ''Prediction of alignment using empirical correction factors'').

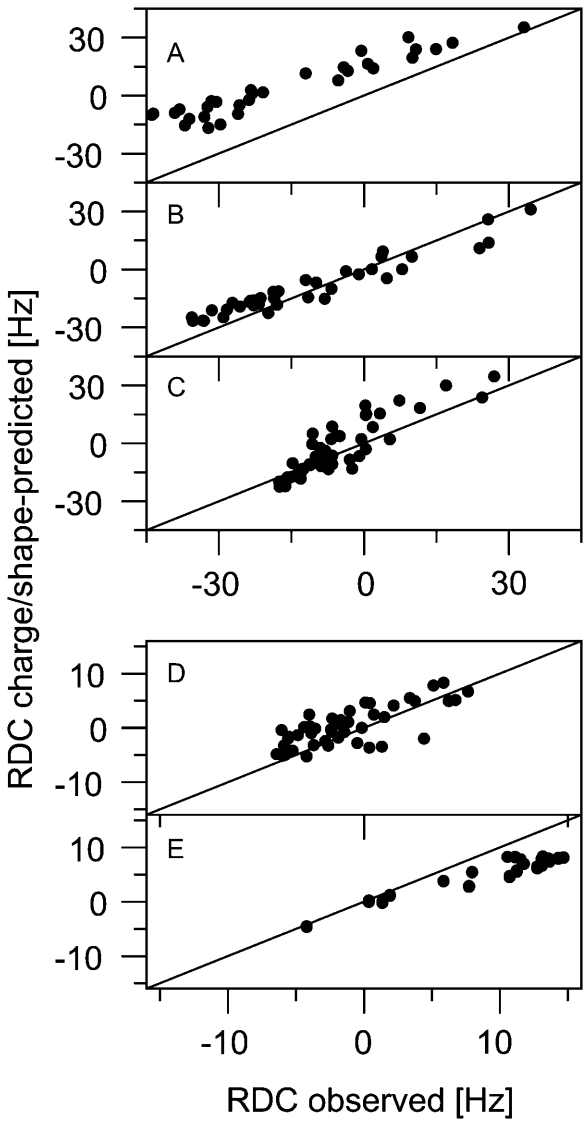

FIGURE 3 Comparison of experimental $^1D_{NH}$ values with values predicted on the basis of the molecules' three-dimensional shapes and charge distributions (taking into account electrostatic effects) for ubiquitin (*A*), DinI (*B*), GB3 (*C*), GB1 (*D*), and the Dickerson dodecamer (*E*). For other details, see legend to Fig. 2.

Influence of structural quality

Fig. 4 demonstrates that our shape/charge model predicts the orientation of electrostatically induced molecular alignment tensors of ubiquitin, DinI, and the Dickerson dodecamer quite well. On the other hand, for both protein G domains a significantly lower prediction quality is achieved. However, it is not clear a priori whether this lower performance for the protein G domains is caused by a shortcoming of our model, or whether prediction for these latter, relatively weakly aligning proteins, is a stronger function of the location of their electrostatic surface charges, whose precise positions generally are dynamically averaged and poorly known. As discussed below, the uncertainty in the precise

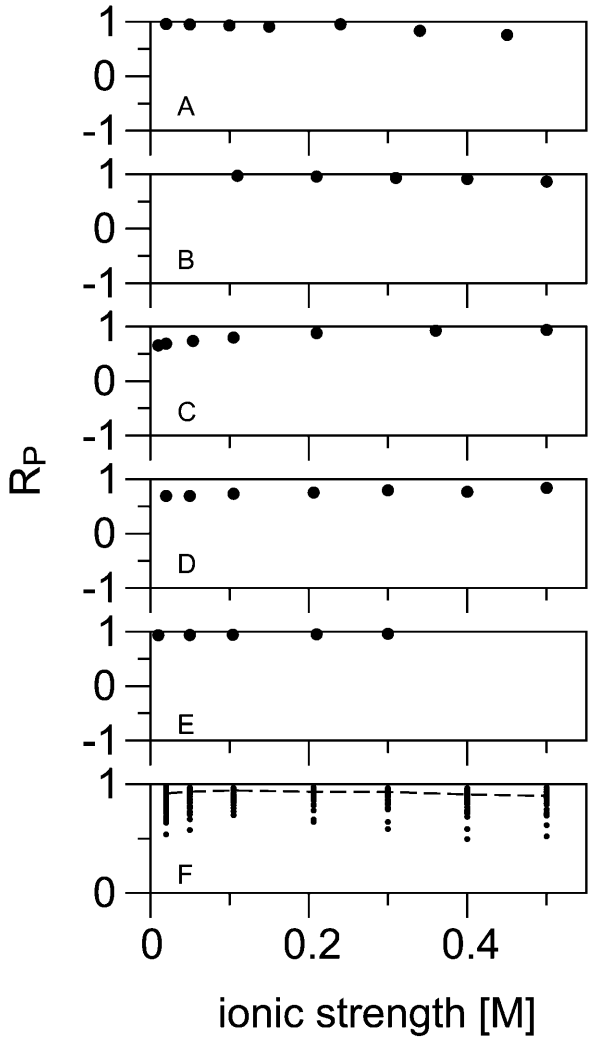

FIGURE 4 Correlation between experimental $^1D_{NH}$ values and charge/shape-predicted couplings. Results for five molecules with very different electrostatic properties are shown: (*A*), ubiquitin; (*B*), DinI; (*C*), GB3; (*D*), GB1; and (*E*), Dickerson dodecamer. In (*F*) the charge/shape prediction results for the ensemble of 3GB1 structures is shown. Dashed line indicates R_P values for the regularized average structure of the ensemble. Alignment magnitudes are presented in Fig. 7.

surface charge locations modulates the alignment orientation by amounts comparable to the deviations between predicted and observed alignment magnitude, suggesting that, particularly for systems such as the GB1 and GB3 domains, with relatively small dipole and quadrupole moments (vide infra), such structural uncertainty introduces errors that are at least comparable to those inherent in the simplifications of our model.

A first indication of the sensitivity of charge/steric predictions to the conformation of charged side chains is seen when evaluating prediction results for the entire ensemble of 20 NMR structures of DinI deposited in the Protein Data Bank (PDB). Despite the low root mean-square (RMS) spread of the highly refined structure (0.17 Å for the backbone, and 0.84 Å for all atoms) and the high quality of backbone cross-validation and Ramachandran map statistics, a considerable degree of variation in the alignment orientation and magnitude is observed among these 20 members of the ensemble (Fig. 5). In particular, two of the 20 NMR models result in a significantly worse prediction, with $R_P = 0.88$ (compared to an average value of 0.96). Despite the high quality and small RMS spread of the backbone structure, there is considerable variation in the predicted alignment magnitude, too. It covers a D_a(NH) range from 13 to 26 Hz, with an average value of 19.7 Hz. The lowest RDC correlation factor, $R_P = 0.88$, is obtained for model 15 of the NMR ensemble (PDB code: 1GHH; Ramirez et al., 2000). It can be traced back to a change in the χ_1 angle for Lys^{57}. Adjusting the single χ_1 angle of Lys^{57} to $-60°$ (as observed in most of the other NMR structures) increases R_P to 0.95.

The spread in predicted alignment caused by slight variations in protein structure is even more dramatic for GB3 and GB1, which have smaller dipole and quadrupole moments than DinI (Table 2). As a result, small changes in

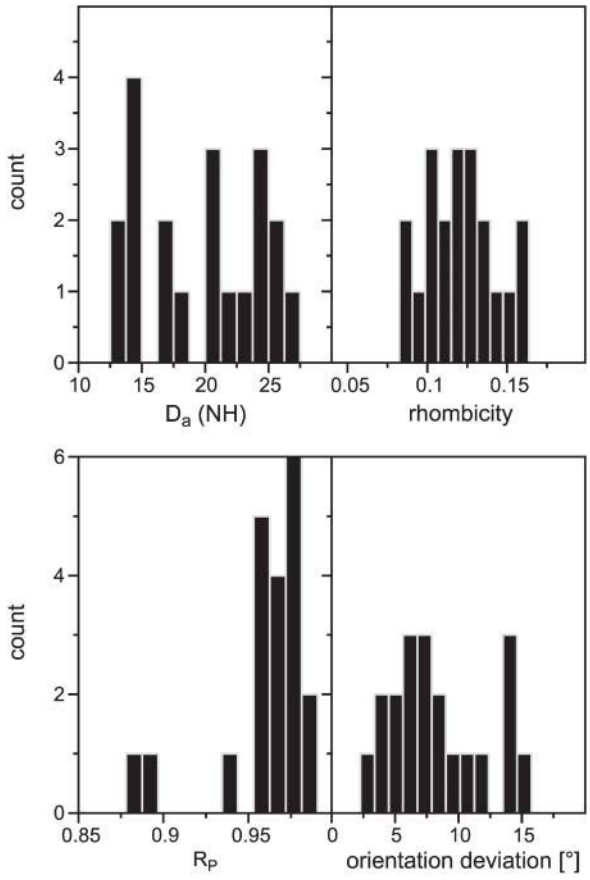

FIGURE 5 Distribution in magnitude, D_a(NH), rhombicity, D_r/D_a, dipolar coupling correlation, R_P, and orientation of charge/shape-predicted alignment tensors, resulting from small structural differences across the NMR ensemble of 20 DinI structures (PDB code: 1GHH) at 0.20 M NaCl, pH 7. The prediction quality is evaluated using Pearson's linear correlation factor, R_P. The deviation in orientation is expressed as a generalized angle, according to Sass et al. (1999).

TABLE 2 Monopole, dipole, and quadrupole moment of the five molecules investigated

System studied	Monopole (e)	Dipole (Debye)	G_{Mag}(Quad)* ($\times$ 10^{-3}) (Å^{2}e)
Ubiquitin	0.33	290	0.8
DinI	−4.67	400	5.5
GB3	−2.00	200	1.8
GB1	−4.00	80	1.4
Dickerson dodecamer	−22.00	0	5.3

*The magnitude of the quadrupole moment, G_{Mag}(Quad), is calculated after diagonalization of the symmetric, traceless quadrupole tensor using $G_{Mag}(\text{Quad}) = 2Q_a[\pi(4 + 3(Q_r/Q_a)^2)/5]^{1/2}$, where Q_a and Q_r are the axial and rhombic components, respectively, of the quadrupole tensor.

the position of charged groups on the protein surfaces have larger relative effects on the orientation and magnitude of their dipole and quadrupole orientation and magnitudes. Generation of alternate GB3 models by subjecting the x-ray structure to a brief molecular dynamics run resulted in structures that deviate by <0.95 Å for all non-H atoms. Calculation of the predicted dipolar couplings at 200 mM NaCl yields correlation coefficients, R_P, relative to observed values that range from 0.68 to 0.97. A similar test for GB1 yields R_P values in the 0.45–0.96 range.

Additional support for the importance of side-chain conformations for the electrostatic alignment of GB1 comes from a charge/shape prediction analysis of GB1 with a new NMR structure. That structure was recently refined with a large number of residual dipolar couplings (PDB code: 3GB1). Performing a PALES prediction with the regularized average structure of the ensemble of 3GB1 structures results in correlation factors, R_P, between experimental and predicted RDCs ≥0.89 across the whole salt range. Remarkably, when considering all members of the NMR ensemble, very large variations in R_P are observed (Fig. 4 *F*) despite the small coordinate RMS deviation (RMSD) (1.02 Å for all non-H atoms), indicating that at least for this protein, the error in prediction is dominated by the uncertainty in the coordinates, and not by shortcomings of the model.

Multipole expansion of protein charge distribution

Results obtained for the highly negatively charged Dickerson dodecamer (net charge −22 e), however, indicate some problems with our simple model. Although the orientation of the alignment tensor is accurately predicted (RDC correlation $R_P = 0.95$), the alignment magnitude is underestimated by about a factor of 2 (Fig. 3 *E*). Similarly, dipolar couplings predicted for ubiquitin—although much improved compared to a pure obstruction model—still underestimate experimentally observed values (Fig. 3 *A*).

To investigate the differences between predicted and experimental alignment magnitudes and to find out which electrostatic interactions are most important for molecular ordering, we dissected the electrostatic contribution to molecular alignment into its multipole components, up to third order. The quadrupole tensor $\mathbf{Q} = (Q_{\alpha\beta})$ with $\alpha, \beta = 1, 2, 3$ of a set of point charges q_i ($i = 1, \ldots, N$) at positions $\mathbf{r}_i = (x_i, y_i, z_i)^T$ is defined as

$$Q_{\alpha\beta} = \sum_{i=1}^{N} q_i(3r_{i\alpha}r_{i\beta} - \delta_{\alpha\beta}r_i^2) \tag{5}$$

where $r_{i1} = x_i$, $r_{i2} = y_i$, $r_{i3} = z_i$, and $r_i^2 = x_i^2 + y_i^2 + z_i^2$. $\delta_{\alpha\beta}$ is the Kronecker delta which is 1 for $\alpha = \beta$ and zero otherwise. Note that the trace of $\mathbf{Q}$ is zero, $Tr(\mathbf{Q}) = \sum_{\alpha=1}^{3} \boldsymbol{Q}_{\alpha\alpha} = 0$. The positions of the charges $\mathbf{r}_i$ in Eq. 5 are given with respect to a reference center. The center defines the origin of the Cartesian coordinate system. If the charge distribution has a nonzero net charge $q = \sum_{i=1}^{N} q_i$, or a nonzero dipole moment, $\mu = \sum_{i=1}^{N} q_i\mathbf{r}_i$, then the quadrupole tensor $\mathbf{Q}$ is not uniquely defined, i.e., it depends on the choice of the reference center. In all calculations below, the reference center is chosen to coincide with the center of mass.

To calculate the electrostatic interaction energy of a quadrupolar system in an external electrostatic potential $\varphi(\mathbf{r})$, we seek to replace the quadrupole moment of all charges q_i with a simpler set of charges that has the same quadrupolar tensor and no net charge and dipole moment. First, we calculate the eigenvalues λ_x, λ_y, and λ_z of $\mathbf{Q}$ with corresponding orthonormal eigenvectors $\mathbf{v}_x$, $\mathbf{v}_y$, and $\mathbf{v}_z$, such that

$$\begin{pmatrix} \nu_x^T \\ \nu_y^T \\ \nu_z^T \end{pmatrix} \mathbf{Q}\left(\boldsymbol{\nu}_x\boldsymbol{\nu}_y\boldsymbol{\nu}_z\right) = \begin{pmatrix} \lambda_x & 0 & 0 \\ 0 & \lambda_y & 0 \\ 0 & 0 & \lambda_z \end{pmatrix}, \tag{6}$$

with

$$\lambda_x + \lambda_y + \lambda_z \equiv 0$$

and

$$\boldsymbol{Q} = \sum_{\gamma=1}^{3} \lambda_\gamma \boldsymbol{\nu}_\gamma \boldsymbol{\nu}_\gamma^T, \tag{7}$$

i.e., $Q_{\alpha\beta} = \sum_{\gamma=1}^{3} \lambda_\gamma \nu_{\gamma\alpha}\nu_{\gamma\beta}$, where $\gamma = 1$, 2, and 3 correspond to x, y, and z. One can then place charges q_x at $\pm\ \varepsilon\mathbf{v}_x$, q_y at $\pm\ \varepsilon\mathbf{v}_y$, q_z at $\pm\ \varepsilon\mathbf{v}_z$ and $-2(q_x + q_y + q_z)$ at the origin (i.e., the reference center, for example the center of mass). This neutral arrangement of seven charges has the same quadrupole tensor $\mathbf{Q}$, and a vanishing dipole moment, if

$$\begin{aligned} q_x &= \lambda_x/(6\varepsilon^2) \\ q_y &= \lambda_y/(6\varepsilon^2) \\ q_z &= \lambda_z/(6\varepsilon^2) \end{aligned}. \tag{8}$$

The electrostatic interaction energy U of the seven charges with the external field $\varphi(\mathbf{r})$ is then:

$$U = \left\{ \begin{array}{l} q_x\varphi(\mathbf{r} - \varepsilon\mathbf{v}_x) - 2q_x\varphi(\mathbf{r} + 0) + q_x\varphi(\mathbf{r} + \varepsilon\boldsymbol{\nu}_x) + \\ q_y\varphi(\mathbf{r} - \varepsilon\mathbf{v}_y) - 2q_y\varphi(\mathbf{r} + 0) + q_y\varphi(\mathbf{r} + \varepsilon\boldsymbol{\nu}_y) + \\ q_z\varphi(\mathbf{r} - \varepsilon\mathbf{v}_z) - 2q_z\varphi(\mathbf{r} + 0) + q_z\varphi(\mathbf{r} + \varepsilon\boldsymbol{\nu}_z) \end{array} \right\}. \quad (9)$$

In the limit of $\varepsilon \rightarrow 0$, Eq. 9 reduces to an expression in terms of the electric field gradient <EFG>. Here, an appropriate choice for the distance from the center is $\varepsilon = 1$ Å.

Fig. 6 shows the correlation between experimental RDCs and those predicted based on a model that takes into account all protein/DNA atoms for evaluation of steric obstruction with the liquid crystal particle, but uses a simplified model for the charge distribution of the biomolecule. In this simplified electrostatic model the charge distribution is reduced to only the monopole q (*dashed lines*), only the dipole μ (*dotted lines*), only the quadrupole **Q** (*dash-dot-dash lines*), or to a combination of all three multipole moments (*solid lines*). As expected, it is not sufficient to consider only the monopole component. Electrostatic interactions with the directionless monopole affect the orientational distribution of the solute only by reweighting the distance distribution with respect to the charged surface, and thus predominantly influence the alignment magnitude and not the orientation of a molecular alignment tensor. The residual correlation observed in Fig. 6, especially at high salt, is due to the nonzero steric contribution to alignment.

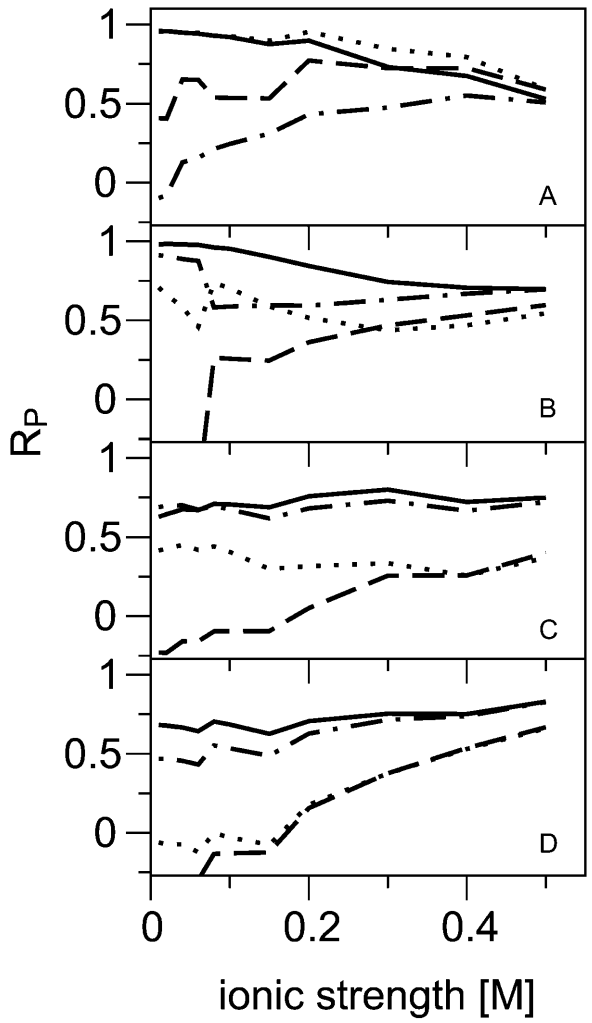

FIGURE 6 Correlation between experimental $^1D_{NH}$ values and charge/shape-predicted couplings as a function of ionic strength for increasing complexity of the charge model used for biomolecules. In the simplified electrostatic model the charge distribution is reduced to only the monopole q (*dashed lines*), only the dipole μ (*dotted lines*), only the quadrupole **Q** (*dash-dot-dash lines*), or to a combination of all three multipole moments (*solid lines*). Results are shown for four proteins: (*A*), ubiquitin; (*B*), DinI; (*C*), GB3; (*D*) GB1.

Is it sufficient to consider the biomolecule just as a dipole or a quadrupole? For ubiquitin the orientation of the experimental alignment tensor is reasonably well reproduced across most of the ionic strength when just the dipole moment is taken into account (Fig. 6 *A*). For GB3, on the other hand, RDCs predicted based on the dipole moment agree relatively poorly with experimental values. For this protein, representation of its electrostatic properties by a quadrupole moment seems more appropriate (Fig. 6 *C*). For DinI and GB1, neither the dipole nor the quadrupole representation alone is sufficient, and only when all three multipole moments are taken into account do the predicted dipolar couplings correlate with experimental values. Remarkably, for all four proteins the orientation of the alignment tensor is reasonably well reproduced across the whole salt range when the molecule is represented by a monopole/dipole/quadrupole model, i.e., when its electrostatic properties are represented by ten pseudocharges that have the same monopole, dipole, and quadrupole moment as all charged side chains (backbone phosphates) taken together. Higher multipoles, therefore, are unlikely to play a major role for molecular ordering. This agrees with the increasingly short-range interaction range of higher multipoles. Nevertheless, the slightly more accurate predictions by the full charge model (Fig. 4 versus *solid lines* in Fig. 6) indicate that treating side-chain charges in atomic detail leads to better results than the multipole decomposition approach in which all side-chain charges are represented by only ten pseudocharges located at the geometric center of the molecule. This result is not unexpected as the multipole expansion is only valid for distances between the liquid crystal particle and the molecule that are large compared to the spatial extension of the molecule's charge distribution.

Similar conclusions are obtained from the relative magnitude of alignment that each multipole moment contributes to the total alignment strength. Alignment of biomolecules in charged liquid crystals is generally a function of all three multipole moments. Moreover, their relative importance seems to depend on ionic strength with the quadrupole moment **Q** becoming more important at higher salt concentrations (data not shown).

Empirical optimization of multipole contributions

The alignment tensor direction remains close to experimentally observed values for all five molecules across the complete salt range from 0.02 to 0.50 M NaCl (Fig. 4). However, as mentioned before, the alignment magnitude of the Dickerson dodecamer is underestimated by about a factor of 2 (Fig. 3 *E*) using the full charge distribution. In addition, outside of the 0.10 to 0.20 M salt range, alignment magnitudes predicted for DinI, ubiquitin, GB3, and GB1 tend to scale incorrectly with ionic strength, but to different degrees for different proteins. For ubiquitin the full charge model overestimates alignment magnitude at low ionic strength, whereas for the other proteins it is underestimated (*solid gray line* in Fig. 7). Ubiquitin is the only one of the four proteins that possesses a positive net charge at pH 7 ($q = 0.33$ e), suggesting that electrostatic attraction and repulsion are overestimated in our calculations. For DinI, on the other hand, the alignment magnitude is underestimated at high salt concentrations, pointing to incorrect weighting of the dipole and quadrupole moments. To evaluate whether these deviations can be corrected for empirically, we introduce scale factors kM, kD, and kQ by which the pseudocharges of the monopole, the dipole, and the quadrupole moment, respectively, are multiplied. Thus, if we want to decrease the influence of the monopole, we have to multiply the pseudocharge that is placed at the geometric center of the molecule (with a value of 0.33 e for ubiquitin) by a factor smaller than 1. As we have three different variables (kM, kD, and kQ) and five different molecules, optimum scale factors were determined with a three-dimensional grid search. kM, kD, and kQ were varied independently from $1/k$ to k with $k = 3$ and a step size for k of 0.2. For each of the 9261 $\{kM, kD, kQ\}$ combinations, charge/shape predictions are made for all five molecules. All $\{kM, kD, kQ\}$ combinations were ranked according to the overall, normalized RMSD between experimental and charge/shape-predicted RDCs, calculated for the five molecules. The $\{kM, kD, kQ\}$ combination with the lowest overall RMSD (sum of individual protein RMSDs normalized by each protein's magnitude of alignment) is therefore the one that best reproduces both the magnitude and the orientation of the alignment tensor for all five molecules. According to Fig. 6 the scale factors will also depend on the ionic strength. Therefore, the grid search is repeated for seven salt concentrations, ranging from 0.02 to 0.50 M NaCl. The weight factors that optimize agreement between observed and predicted dipolar couplings are listed in Table 3.

Prediction of alignment using empirical correction factors

Fig. 7 compares the magnitude of experimental alignment tensors with values predicted by the multipole model introduced above. In the multipole model the pseudocharges for the monopole, dipole, and quadrupole are scaled by the optimized, empirical scale factors kM, kD, and kQ, respectively, that were obtained from the grid search. The corresponding correlation coefficients between observed and predicted dipolar coupling values are shown in Fig. 8.

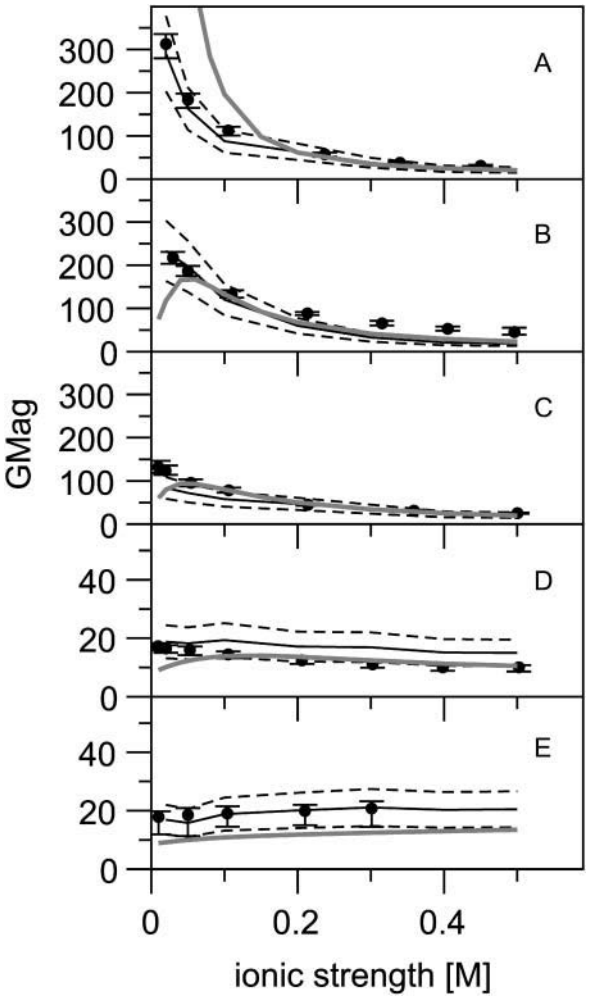

FIGURE 7 Dependence of alignment magnitude on ionic strength for ubiquitin (*A*), DinI (*B*), GB3 (*C*), GB1 (*D*), and the Dickerson dodecamer (*E*). Filled symbols mark values obtained from experimental dipolar couplings by SVD. Error bars represent the influence of structural noise on SVD calculations (Zweckstetter and Bax, 2002). Solid gray lines represent the alignment magnitudes for the full electrostatic model without multipole scaling using the following structures: (*A*), 1D3Z; (*B*), 1GHH; (*C*), residue 6-61 of 1IGD; (*D*), 1PGA; and (*E*), 1DUF. Solid black lines correspond to the charge/shape predictions that were obtained with empirically optimized scaling factors for the monopole, dipole, and quadrupole moment (see text). Error estimates (*dotted lines*) are standard deviations obtained from the ensemble of NMR structures (A,B) and amount to roughly 30%. The alignment magnitude, G_{Mag}, is defined in Eq. 1. To facilitate comparison with the familiar D_{a}(NH) values, G_{Mag} values have been multiplied by $D_{\mathrm{max}}^{\mathrm{NH}} = 21,585$ Hz.

At pH 7, ubiquitin has a net positive charge ($q = 0.33$ e) and a large dipole moment ($\mu \approx 290$ Debye) causing very strong ordering in negatively charged Pf1 (Fig. 7 *A*). Decreasing the ionic strength from 0.50 M to 0.02 M NaCl increases the alignment magnitude by one order of magnitude. The ordering strength increases for two reasons.

TABLE 3 Grid search-derived optimal scale factors for the electric monopole, dipole, and quadrupole moments as a function of ionic strength

NaCl (mM)	*k*M	*k*D	*k*Q
20	0.45	0.7	1.0
50	0.45	0.8	0.8
100	0.42	1.0	0.8
200	0.45	1.6	0.8
300	0.7	2.0	1.2
400	1.0	2.2	1.4
500	1.4	2.8	1.8

First, the magnitude of the negative surface potential adjacent to the liquid crystal particle increases at lower salt concentrations. Second, decreasing the ionic strength from 0.50 M to 0.02 M NaCl increases the Debye length from 0.4 to 2.1 nm (Fig. 9 *B*) and more molecules can contribute to alignment. The orientation of the alignment tensor stays nearly unchanged when going from 0.02 to 0.50 M NaCl, as evidenced by the high R_P between dipolar couplings observed at low and high ionic strength (*dashed lines* in Fig. 8 *A*). This indicates that electrostatics dominate across the whole range of ionic strengths accessible to NMR, in agreement with our model.

Results similar to those for ubiquitin are found for DinI ($q = -4.67$ e; $\mu \approx 400$ Debye) and GB3 ($q = -2.0$ e; $\mu \approx 200$ Debye). However, due to its net negative charge, the increase in alignment magnitude at low ionic strength is less pronounced (Fig. 7, *B* and *C*) and both the predicted and observed alignment orientations change with salt concentration (*dashed curves* in Fig. 8, *B* and *C*). In the case of DinI, a small underestimation of the experimental alignment magnitude remains at high salt concentrations, despite introduction of the empirical scale factors.

GB1 ($q = -4.0$ e; $\mu \approx 80$ Debye) shows a much weaker dependence of alignment strength on salt concentration than DinI and GB3. Although it differs from GB3 by only three charged residues the alignment magnitude decreases by just 40% when going from 0.02 to 0.50 M NaCl (Fig. 7 *D*). In addition, for salt concentrations above 0.15 M NaCl the steric component of the alignment tensor plays a significant role. This causes an experimentally observed rotation of the alignment tensor orientation by ~60° when going from 0.02 to 0.50 M NaCl. Accordingly, experimental dipolar couplings measured at 0.02 M NaCl and at 0.50 M NaCl correlate poorly with one another ($R_P = 0.44$). The quality of charge/shape-predicted dipolar couplings in GB1, on the other hand, remains high across the entire salt range and even increases at high ionic strength (Fig. 8 *D*). This demonstrates that the increasing steric contribution to alignment is correctly taken into account by our simple model. As discussed earlier, the overall lower correlation for the protein G domains compared to ubiquitin and DinI can be attributed largely to differences in side-chain orientation when using a static x-ray model to describe the solution structure.

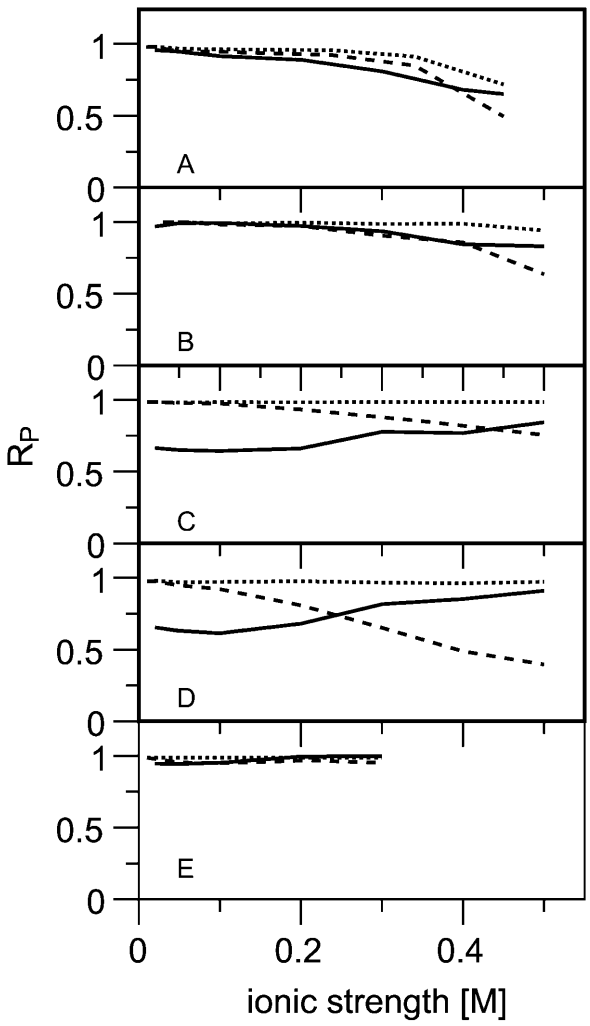

FIGURE 8 Correlation between experimental $^1D_{NH}$ values and charge/shape-predicted couplings (*solid lines*), or SVD best-fit couplings (*dotted lines*) as a function of ionic strength. The dashed lines indicate the correlations between experimental couplings at a certain ionic strength and those observed at low salt (~0.02 M NaCl). Results for five molecules with very different electrostatic properties are shown: (*A*), ubiquitin; (*B*), DinI; (*C*), GB3; (*D*), GB1; and (*E*), Dickerson dodecamer. Note that for ubiquitin, at the low Pf1 concentrations used, the drop in R_P above 0.30 M NaCl is dominated by the reduced relative accuracy of dipolar couplings. Note that these results were obtained with empirically optimized scaling factors for the monopole, dipole, and quadrupole moment (see text).

Figs. 7 *E* and 8 *E* show the results of charge/shape prediction for a very highly charged molecule, the Dickerson dodecamer ($q = -22$ e). As discussed earlier, the orientation of the simulated alignment tensor remains unchanged when going from 0.01 to 0.30 M NaCl, in agreement with experimental results. In addition, experimental and simulated RDCs are highly correlated, with a Pearson's correlation factor of 0.96, demonstrating that the orientation of the alignment tensor is correctly predicted.

Remarkably, both our model and the experimental results indicate very little dependence of alignment magnitude on ionic strength. In contrast to the four proteins, the alignment

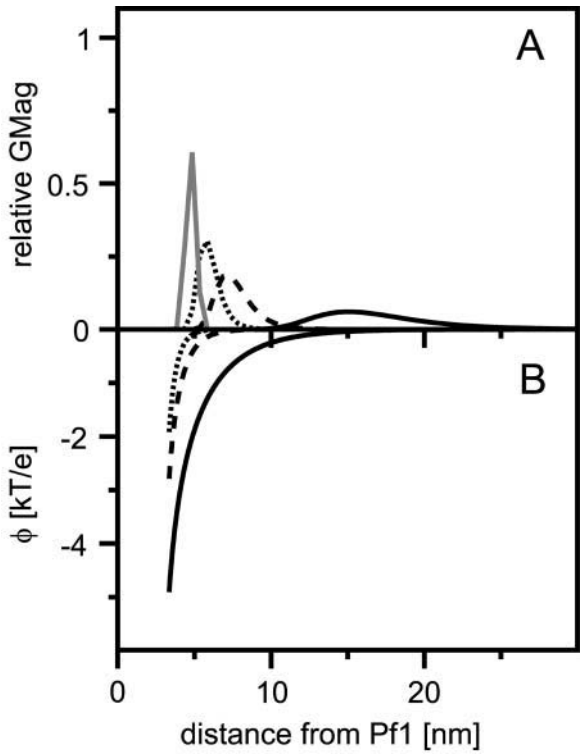

FIGURE 9 (*A*) Magnitude of DNA dodecamer alignment relative to the total alignment magnitude, as a function of distance between the center of gravity of the dodecamer and the axis of the viral rod, calculated using shells of 5 Å thickness for various ionic strengths. The *x* axis indicates the distance from the center of a Pf1 rod to the inner surface of the 5 Å shell. Different NaCl concentrations are indicated in the following way: solid line, 0.01 M; dashed line, 0.1 M; and dotted line, 0.3 M. In gray, the shell distribution for the steric case is shown. (*B*) Electrostatic potentials of bacteriophage Pf1, using a cylinder radius of 3.35 nm and a surface charge density of −0.475 e/nm^2, calculated from the nonlinear Poisson-Boltzmann equation at 0.01 M (*solid line*), 0.1 M (*dashed line*), and 0.3 M (*dotted line*) NaCl.

magnitude of the DNA does not decrease with increasing salt concentration. It actually shows a small increase (~15%) when going from 0.01 to 0.30 M NaCl (Fig. 7 *E*). This increase in alignment magnitude can be rationalized by evaluating how much of the total alignment is contributed by molecules as a function of distance from the center of the Pf1 rod. To this extent, we calculated the percentage of total alignment that comes from molecules for which the center of gravity is located within shells of 5 Å thickness, for example within distances ranging from 60 to 65 Å from the Pf1 rod (Fig. 9). No alignment comes from positions very close to the Pf1 particle, as all possible orientations are sterically forbidden. As soon as the molecule is far enough away and orientations exist that are not sterically forbidden, the contribution to overall alignment quickly rises, reaches a maximum, and then drops to zero. If only steric effects are considered, the contributing region is restricted to translational positions where obstruction between the molecule and the hard-wall potential can occur. Outside this region all orientations are equally probable and no preferred orientation exists (shown in *gray*). When electrostatic interactions are taken into account, the free energy of the protein is orientation-dependent and the main contribution to alignment comes from outside the steric overlap region. The position of the maximum depends on ionic strength: the lower the salt concentration the further away is the shell from the Pf1 rod that contributes the most to ordering. Distances closer to the phage are unfavorable as electrostatic repulsion between the highly negatively charged DNA and Pf1 dominates. Thus, the increase in alignment before it drops to zero results from the initial increase in the number of molecules per shell as a function of the distance from the Pf1 surface, whereas the drop-off in G_{Mag} per shell initially is small. The same argument explains the Dickerson dodecamer's increase in alignment magnitude with increasing salt concentration: at higher ionic strength, more molecules are close to the Pf1 particle, enabling a bigger contribution to alignment by steric obstruction.

DISCUSSION

Electrostatic model

Our model only takes into account short-range steric and long-range electrostatic interactions. Nonpolar interactions, such as a Born repulsion and a nonpolar attraction, are neglected. This simplification was motivated by the fact that previous studies have shown that the two opposing nonpolar interactions approximately balance each other (BenTal et al., 1997). In addition, whereas the long-range electrostatic interaction does not significantly depend on the atomic details of the liquid crystal surface, both nonpolar interactions—as they become important when the solute approaches the liquid crystal particle—strongly depend on the model used for the liquid crystal surface. Thus, to include nonpolar interactions, the liquid crystal particle would need to be represented in atomic detail. The good agreement between experimental and predicted alignment tensor values obtained in our study demonstrates that such nonpolar effects at most play a minor role.

There are at least four other simplifications that enter our treatment of electrostatic effects:

1. The molecular solvent—water and ions—is treated at the continuum level, thus excluding the possibility of specific molecular interactions such as ion binding to the protein or phage surface. Although simulation studies of simple models of ions near polyelectrolytes have shown reasonable agreement with such continuum descriptions (Mills et al., 1985; Murthy et al., 1985), we expect deviations in the limits of (a), close contact between protein and interface; (b), low salt concentrations resulting in tight ionic interactions; and (c), high salt concentrations where ion packing contributions play a role. The effects of multivalent and molecular ions are also expected to be described relatively poorly by the simple PB continuum model.

2. The orientation-dependent interactions of the protein with the charged interface are calculated by using the electrostatic potential of the unperturbed interface, without calculating the combined effect of protein and interface on the distribution of ions in their vicinity.
3. Although our model explicitly treats the shape and charge distribution of the solute, the charge distribution on the liquid crystal particle is assumed to be uniform. This approximation is expected to lead to errors when the protein is close to the interface, where specific interactions with interfacial charge distribution are important.
4. The protein structure and the charge distribution on the protein and interface are assumed to be rigid and independent of orientation and distance. Errors are expected for proteins with flexible charged side chains that can adjust their conformation to optimize electrostatic interactions with the interface.

   However, the reasonably quantitative agreement between observed and predicted alignment suggests that the above simplifications do not have dramatic adverse effects on the values predicted by our simplified model.

The effect of transient binding of the solute to the liquid crystal particle is negligible. If such transient binding occurred, it could introduce important contributions from higher multipole terms as well as nonlinear interaction of separate steric and electrostatic contributions. However, from an NMR perspective, the liquid crystal particle behaves like a solid, and transient binding to it would dramatically increase its transverse relaxation rates, contrary to what is seen for the majority of proteins dissolved in such systems. Even in cases where apparent line broadening in Pf1 medium is observed (DinI and ubiquitin <0.1 M NaCl), such line broadening frequently results from large residual dipolar couplings, whereas ^{15}N relaxation rates are nearly unchanged compared to isotropic solutions. However, at low ionic strength an increase in the ^{15}N transverse relaxation rate is observed for ubiquitin (data not shown), together with very strong alignment of the protein, indicating that in this case transient binding events are no longer negligible.

Surface charge of liquid crystal particles

For applying our charge/shape model to structure determination of biomolecules, a potential problem is that the surface charge for many of the liquid crystals is not known accurately and depends on the method of preparation. For example, the charge on the surface of the cellulose-based phase (Fleming et al., 2000) depends on particle size and on the length of acid hydrolysis used. In doped bicelles, protein alignment data indicate a surface charge that is nearly threefold lower than expected on the basis of the mole fraction of added charged amphiphiles, when using an infinite bilayer as the model for the liquid-crystalline medium. The smaller effective charge may result from a preferential partitioning of the charges near or in the rim of the pores, where their effect on solute alignment is very different from those partitioned in the regular bilayer. The same is found for the ostensibly neutral undoped bicelles, where empirically a very small amount of negative charge is found to improve the agreement between predicted and observed dipolar couplings over the purely steric alignment model. The presence of such charge had been predicted (Losonczi and Prestegard, 1998), but the precise magnitude is found to depend on the source of the materials used in the preparation of the liquid crystal. Knowledge of a rather accurate value of the surface charge of the liquid crystal will be important for applications that employ only slightly charged liquid crystals. For such liquid crystals the exact balance between obstruction and electrostatic interaction will determine the orientation and magnitude of the alignment tensor. For highly charged liquid-crystalline media such as bacteriophage Pf1, purple membrane fragments, and cetylpiridinium-based media, on the other hand, exact knowledge of the surface charge of the liquid crystal poses less of a problem. For salt concentrations up to 0.10–0.20 M NaCl, electrostatic interactions will dominate the molecular ordering for most molecules.

Accuracy of charge/shape-predicted alignment tensors

The full charge model, i.e., the model where the protein/nucleic acid is represented by effective charges placed at the positions of its ionizable residues, is superior to the multipole expansion model for predicting the alignment tensor orientation. This is expected, as a multipole decomposition is only valid for distances between the liquid crystal particle and the molecule that are large compared to the spatial extension of the molecule's charge distribution. The magnitude of alignment, on the other hand, is only correctly predicted after replacing the effective charges by a multipole expansion and introduction of empirical scale factors for the monopole, dipole, and quadrupole moment. These empirical scale factors were determined from experimental data obtained for five biomolecules with very different electrostatic properties, and are therefore expected to be applicable to a broad range of proteins and nucleic acids. Nevertheless, the scaling factors must be seen mainly as a compensation tool for the simple nature of our model. The choice of basing these scaling factors on the mono-, di-, and quadrupole moments was made on the basis of their different potential versus distance relationships when varying ionic strength. It cannot be excluded, however, that other empirical parameters could yield equally satisfactory or even better results. Further improvements over our model would require solving the nonlinear PB equation for every distance and orientation of the protein with respect to the surface of the liquid crystal particle.

More importantly, our results indicate that—from the point of application toward structure determination of biomolecules—the accuracy of prediction is ultimately limited by factors other than the details of the electrostatic model. As discussed above, minor rearrangement of the side chains of charged surface residues can dramatically affect the correlation between observed and predicted dipolar couplings. This effect was particularly dramatic for GB1, which has a relatively uniform charge distribution based on its x-ray structure that results in small dipole and quadrupole moments. On the other hand, variation of simulation parameters such as the resolution of the orientational or translational grid, the boundary condition used for calculating the electrostatic potentials, or the detail of the charge distribution, i.e., putting charges only on the side chains of ionizable residues versus using the CHARMM TOPH19 parameter set which puts partial charges on all atoms, has only a small effect on the results obtained from charge/shape prediction. We thus expect that using a more sophisticated and computationally more costly electrostatic model (such as the one implemented in DELPHI; BenTal et al., 1997, 1996; Gallagher and Sharp, 1998; Murray and Honig, 2002; Peitzsch et al., 1995) may only marginally improve the accuracy of predicted alignment tensors—at least not with the quality of three-dimensional structures and their conformational dynamics currently available. NMR relaxation experiments indicate that many of the long side chains of charged residues such as Lys, Arg, and Glu are frequently subject to conformational averaging. In addition, long, flexible, charged N- or C-termini of protein backbones pose a problem for accurate prediction of charge-induced alignment. In principle, it may be possible to use the agreement between observed and charge/shape-based alignment tensor as a restraint when calculating the ensemble, or as a selection criterion when evaluating which ensemble members are acceptable.

From the presented results it is clear that the quality of prediction varies between proteins. This is due to either the oversimplified nature of our model or inaccuracies in the structural model. Therefore, it is difficult to quantitatively evaluate how good a structure is with the simple model introduced here. However, most applications of the charge/steric prediction model (similar to the already widely used steric prediction model) will focus on a distinction between several structural models that are not easily distinguished by other methods. For example, if very different relative conformations (e.g., parallel versus antiparallel) of a homodimeric system are in question, the models are likely to yield very different R_P values. Note that even in the very worst of our cases, outside the limits where reliable data could be expected, $R_P > 0.5$, whereas in the absence of structural information, chances are 50% that $R_P < 0$. For example, if for model (A) $R_P = 0.8$ and for model (B) $R_P = -0.3$ then the protein is very likely of the model (A) type.

Interactions responsible for molecular alignment of biomolecules

There has been much debate about which electrostatic interactions are most important for solute alignment in apolar liquid-crystalline media (Dingemans et al., 2003; Emsley et al., 1991; Photinos et al., 1992; Photinos and Samulski 1993; Syvitski and Burnell, 1997, 2000; Terzis et al., 1996; Vroege and Lekkerkerker, 1992). In aqueous media the situation is fundamentally different as the ion distribution in the solvent dramatically perturbs the electrostatic potential.

For electrostatic interactions, higher multipole orders become increasingly short-range. Therefore, it is expected that the interaction between the average electric field and the solute dipole moment, and the interaction of the average electric field gradient <EFG>with the solute quadrupole **Q,** will dominate solute ordering. In apolar organic liquid crystals, the consensus is that generally the <EFG>-**Q** interaction dominates and permanent dipoles at most have small effects on solute orientations (Syvitski and Burnell, 1997, 2000). This is rationalized by the fact that in apolar nematic phases the first rank order parameter of the liquid crystal is zero (i.e., the mean electric field of the nematic phase is zero). Other investigations, however, indicate that dipole interactions do play a nonnegligible role (Dingemans et al., 2003; Photinos et al., 1992; Photinos and Samulski, 1993).

Our multipole expansion model, which uses all atoms of the biomolecule to evaluate obstruction, but a charge distribution that is reduced to the monopole, dipole, and quadrupole moment, provides some insight into interactions responsible for molecular ordering of biomolecules in aqueous liquid-crystalline media. Neither the dipole interaction nor the <EFG>-**Q** interaction alone explains experimental dipolar couplings observed for the four proteins. For ubiquitin, the only one of the four proteins with a net positive charge at pH 7, the interaction of the dipole moment with the average electric field dominates. For GB3, on the other hand, the quadrupole moment is found to be more important for molecular ordering. Our results also show that the strength of alignment cannot be directly deduced from the net charge of the protein. DinI is the most negatively charged protein, with a net charge of about −4.7 e at pH 7. However, DinI aligns very strongly due to its very large dipole moment of ~400 Debye.

Thus, in aqueous phase both the solute dipole and quadrupole affect the ordering of macromolecules. This indicates a nonvanishing net electric field that interacts with the solute dipole in aqueous liquid-crystalline media. More importantly, the terms interfere with each other.

How to modulate alignment tensor orientations

The above analysis of the individual components contributing to a molecular alignment tensor suggests different ways

for modulating a molecular alignment tensor, which can provide invaluable information for the study of both structure (Al-Hashimi et al., 2000; Delaglio et al., 2000; Ramirez and Bax, 1998) and dynamics (Meiler et al., 2001; Peti et al., 2002). For example, the finding that the relative contributions from the net charge and dipole moments scale differently with ionic strength indicates that varying salt concentration can yield linearly independent contributions. It also suggests that titration of surface side chains can be an important way to change alignment when working in highly charged media such as phages. Finally, the analysis suggests that increasing the ionic strength to values as high as 0.5 M allows the use of highly charged liquid-crystalline media, even for proteins that have a very strong electrostatic interaction with the liquid crystal medium at low to intermediate salt concentrations.

CONCLUDING REMARKS

We have shown that a highly simplified model, combining short-range steric and long-range electrostatic interactions, yields a reasonably good relation between a macromolecule's shape and surface charge and its ordering in charged liquid-crystalline media. This demonstrates that steric and electrostatic interactions together dominate weak alignment of biomolecules in polar liquid-crystalline media.

Our previous model, which took into account only steric interactions, is limited to neutral media such as bicelles and alkyl poly(ethylene glycol)-based liquid crystals (Zweckstetter and Bax, 2000). A number of proteins, however, destructively interact with these media, thereby removing the liquid-crystalline order. The opportunities offered by the previous steric alignment model, such as differentiation of monomeric and homodimeric states (Zweckstetter and Bax, 2000), determination of the relative orientation of protein domains (Bewley and Clore, 2000), and validation of structures of protein complexes (Clore and Schwieters, 2003), were therefore not available for these proteins. The model for prediction of charge-induced molecular ordering that is introduced here extends these novel opportunities from neutral to charged liquid-crystalline media. This therefore makes it applicable to essentially all liquid crystals used in biological NMR to date. At the same time, our results demonstrate the exquisite sensitivity of liquid crystal NMR as a source of experimental data to evaluate descriptions of the electrostatic interactions between proteins and charged surfaces.

We thank Ben Ramirez for preparing DinI and GB3 samples and John Louis for the GB1 sample.

This work was supported by the AIDS Targeted Anti-Viral Program of the Office of the Director of the National Institutes of Health. M.Z. is the recipient of a Deutsche Forschungsgemeinschaft Emmy Noether Fellowship (ZW71/1-3).

REFERENCES

Al-Hashimi, H. M., H. Valafar, M. Terrell, E. R. Zartler, M. K. Eidsness, and J. H. Prestegard. 2000. Variation of molecular alignment as a means of resolving orientational ambiguities in protein structures from dipolar couplings. *J. Magn. Reson.* 143:402–406.

Almond, A., and J. B. Axelsen. 2002. Physical interpretation of residual dipolar couplings in neutral aligned media. *J. Am. Chem. Soc.* 124:9986–9987.

Antosiewicz, J., J. A. McCammon, and M. K. Gilson. 1994. Prediction of pH-dependent properties of proteins. *J. Mol. Biol.* 238:415–436.

Azurmendi, H. F., and C. A. Bush. 2002. Conformational studies of blood group A and blood group B oligosaccharides using NMR residual dipolar couplings. *Carbohydr. Res.* 337:905–915.

Barrientos, L. G., C. Dolan, and A. M. Gronenborn. 2000. Characterization of surfactant liquid crystal phases suitable for molecular alignment and measurement of dipolar couplings. *J. Biomol. NMR.* 16:329–337.

Barrientos, L. G., J. M. Louis, and A. M. Gronenborn. 2001. Characterization of the cholesteric phase of filamentous bacteriophage fd for molecular alignment. *J. Magn. Reson.* 149:154–158.

BenTal, N., B. Honig, C. Miller, and S. McLaughlin. 1997. Electrostatic binding of proteins to membranes. Theoretical predictions and experimental results with charybdotoxin and phospholipid vesicles. *Biophys. J.* 73:1717–1727.

BenTal, N., B. Honig, R. M. Peitzsch, G. Denisov, and S. McLaughlin. 1996. Binding of small basic peptides to membranes containing acidic lipids: theoretical models and experimental results. *Biophys. J.* 71: 561–575.

Bewley, C. A. 2001. Rapid validation of the overall structure of an internal domain-swapped mutant of the anti-HIV protein cyanovirin-N using residual dipolar couplings. *J. Am. Chem. Soc.* 123:1014–1015.

Bewley, C. A., and G. M. Clore. 2000. Determination of the relative orientation of the two halves of the domain-swapped dimer of cyanovirin-N in solution using dipolar couplings and rigid body minimization. *J. Am. Chem. Soc.* 122:6009–6016.

Chapman, D. L. 1913. A contribution to the theory of electrocapillarity. *Philosoph. Magaz.* 25:475–481.

Clore, G. M., and C. D. Schwieters. 2003. Docking of protein-protein complexes on the basis of highly ambiguous intermolecular distance restraints derived from 1H/15N chemical shift mapping and backbone 15N-1H residual dipolar couplings using conjoined rigid body/torsion angle dynamics. *J. Am. Chem. Soc.* 125:2902–2912.

Clore, G. M., M. R. Starich, and A. M. Gronenborn. 1998. Measurement of residual dipolar couplings of macromolecules aligned in the nematic phase of a colloidal suspension of rod-shaped viruses. *J. Am. Chem. Soc.* 120:10571–10572.

Cornilescu, G., J. L. Marquardt, M. Ottiger, and A. Bax. 1998. Validation of protein structure from anisotropic carbonyl chemical shifts in a dilute liquid crystalline phase. *J. Am. Chem. Soc.* 120:6836–6837.

Davis, M. E., and J. A. McCammon. 1990. Electrostatics in biomolecular structure and dynamics. *Chem. Rev.* 90:509–521.

Debye, P., and E. Hueckel. 1923. Zur Theorie der Elektrolyte. I. Gefrierpunktserniedrigung und verwandte Erscheinungen. *Phys. Zeitschr.* 24:185–206.

Delaglio, F., S. Grzesiek, G. W. Vuister, G. Zhu, J. Pfeifer, and A. Bax. 1995. NMRPIPE—a multidimensional spectral processing system based on unix pipes. *J. Biomol. NMR.* 6:277–293.

Delaglio, F., G. Kontaxis, and A. Bax. 2000. Protein structure determination using molecular fragment replacement and NMR dipolar couplings. *J. Am. Chem. Soc.* 122:2142–2143.

Derrick, J. P., and D. B. Wigley. 1994. The 3rd Igg-binding domain from streptococcal protein-G—an analysis by x-ray crystallography of the structure alone and in a complex with FAB. *J. Mol. Biol.* 243: 906–918.

Dickerson, R. E., and H. R. Drew. 1981. Structure of a B-DNA dodecamer. II. Influence of base sequence on helix structure. *J. Mol. Biol.* 149:761–786.

Dingemans, T., D. J. Photinos, E. T. Samulski, A. F. Terzis, and C. Wutz. 2003. Ordering of apolar and polar solutes in nematic solvents. *J. Chem. Phys.* 118:7046–7061.

Eisenberg, D., and A. D. McLachlan. 1986. Solvation energy in protein folding and binding. *Nature*. 319:199–203.

Eisenhaber, F., and P. Argos. 1993. Improved strategy in analytic surface calculation for molecular systems: handling of singularities and computational efficiency. *J. Comput. Chem.* 14:1272–1280.

Eisenhaber, F., P. Lijnzaad, P. Argos, C. Sander, and M. Scharf. 1995. The double cubic lattice method: efficient approaches to numerical integration of surface area and volume and to dot surface contouring of molecular assemblies. *J. Comput. Chem.* 16:273–284.

Emsley, J. W., W. E. Palke, and G. N. Shilstone. 1991. The inclusion of electrostatic and dispersion interactions into potentials of mean torque for solutes dissolved in uniaxial liquid-crystal solvents. *Liq. Crystals.* 9:643–648.

Fernandes, M. X., P. Bernado, M. Pons, and J. G. de la Torre. 2001. An analytical solution to the problem of the orientation of rigid particles by planar obstacles. Application to membrane systems and to the calculation of dipolar couplings in protein NMR spectroscopy. *J. Am. Chem. Soc.* 123:12037–12047.

Ferrarini, A. 2003. Modeling of macromolecular alignment in nematic virus suspensions. Application to the prediction of NMR residual dipolar couplings. *J. Phys. Chem. B.* 107:7923–7931.

Fleming, K., D. Gray, S. Prasannan, and S. Matthews. 2000. Cellulose crystallites: a new and robust liquid crystalline medium for the measurement of residual dipolar couplings. *J. Am. Chem. Soc.* 122:5224–5225.

Gallagher, K., and K. Sharp. 1998. Electrostatic contributions to heat capacity changes of DNA-ligand binding. *Biophys. J.* 75:769–776.

Gallagher, T., P. Alexander, P. Bryan, and G. L. Gilliland. 1994. Two crystal structures of the B1 immunoglobulin-binding domain of streptococcal protein G and comparison with NMR. *Biochemistry.* 33:4721–4729.

Gouy, D. L. 1910. Sur la constitution de la charge électrique a la surface d'un électrolyte. *Ann. Phys.* 9:457–468.

Gronenborn, A. M., D. R. Filpula, M. Z. Essiz, A. Achari, M. Whitlow, P. T. Wingfield, and G. M. Clore. 1991. A novel, highly stable form of the immunoglobulin binding domain of streptococcal protein G. *Science.* 253:657–661.

Hansen, M. R., L. Mueller, and A. Pardi. 1998. Tunable alignment of macromolecules by filamentous phage yields dipolar coupling interactions. *Nat. Struct. Biol.* 5:1065–1074.

Honig, B., K. Sharp, and A. S. Yang. 1993. Macroscopic models of aqueous solutions: biological and chemical applications. *J. Phys. Chem.* 97:1101–1109.

Hummer, G., L. R. Pratt, and A. E. Garcia. 1998. Molecular theories and simulation of ions and polar molecules in water. *J. Phys. Chem. A.* 102:7885–7895.

Hus, J. C., D. Marion, and M. Blackledge. 2001. Determination of protein backbone structure using only residual dipolar couplings. *J. Am. Chem. Soc.* 123:1541–1542.

Koradi, R., M. Billeter, and K. Wuthrich. 1996. MOLMOL: a program for display and analysis of macromolecular structures. *J. Mol. Graph.* 14: 51–55.

Losonczi, J. A., and J. H. Prestegard. 1998. Improved dilute bicelle solutions for high-resolution NMR of biological macromolecules. *J. Biomol. NMR.* 12:447–451.

Meiler, J., J. J. Prompers, W. Peti, C. Griesinger, and R. Bruschweiler. 2001. Model-free approach to the dynamic interpretation of residual dipolar couplings in globular proteins. *J. Am. Chem. Soc.* 123:6098–6107.

Mills, P., C. F. Anderson, and M. T. Record. 1985. Monte Carlo studies of counterion-DNA interactions. Comparison of the radial distribution of counterions with predictions of other polyelectrolyte theories. *J. Phys. Chem.* 89:3984–3994.

Murray, D., and B. Honig. 2002. Electrostatic control of the membrane targeting of C2 domains. *Mol. Cell.* 9:145–154.

Murthy, C. S., R. J. Bacquet, and P. J. Rossky. 1985. Ionic distributions near polyelectrolytes: a comparison of theoretical approaches. *J. Phys. Chem.* 89:701–710.

Ottiger, M., and A. Bax. 1999. Bicelle-based liquid crystals for NMR measurement of dipolar couplings at acidic and basic pH values. *J. Biomol. NMR.* 13:187–191.

Ottiger, M., F. Delaglio, and A. Bax. 1998. Measurement of J and dipolar couplings from simplified two-dimensional NMR spectra. *J. Magn. Reson.* 131:373–378.

Peitzsch, R. M., M. Eisenberg, K. A. Sharp, and S. McLaughlin. 1995. Calculations of the electrostatic potential adjacent to model phospholipid bilayers. *Biophys. J.* 68:729–738.

Peti, W., J. Meiler, R. Bruschweiler, and C. Griesinger. 2002. Model-free analysis of protein backbone motion from residual dipolar couplings. *J. Am. Chem. Soc.* 124:5822–5833.

Photinos, D. J., C. D. Poon, E. T. Samulski, and H. Toriumi. 1992. NMR study of the effects of electric-dipole interactions on the ordering of chain solutes in the nematic phase. *J. Phys. Chem.* 96:8176–8180.

Photinos, D. J., and E. T. Samulski. 1993. Electric-dipole interactions of chain molecules in nematics—the analysis of segmental ordering in α,ω-dibromoalkanes. *J. Chem. Phys.* 98:10009–10016.

Prestegard, J. H., and A. I. Kishore. 2001. Partial alignment of biomolecules: an aid to NMR characterization. *Curr. Opin. Chem. Biol.* 5:584–590.

Prosser, R. S., J. A. Losonczi, and I. V. Shiyanovskaya. 1998. Use of a novel aqueous liquid crystalline medium for high- resolution NMR of macromolecules in solution. *J. Am. Chem. Soc.* 120:11010–11011.

Ramirez, B. E., and A. Bax. 1998. Modulation of the alignment tensor of macromolecules dissolved in a dilute liquid crystalline medium. *J. Am. Chem. Soc.* 120:9106–9107.

Ramirez, B. E., O. N. Voloshin, R. D. Camerini-Otero, and A. Bax. 2000. Solution structure of DinI provides insight into its mode of RecA inactivation. *Protein Sci.* 9:2161–2169.

Ruckert, M., and G. Otting. 2000. Alignment of biological macromolecules in novel nonionic liquid crystalline media for NMR experiments. *J. Am. Chem. Soc.* 122:7793–7797.

Sass, J., F. Cordier, A. Hoffmann, M. Rogowski, A. Cousin, J. G. Omichinski, H. Lowen, and S. Grzesiek. 1999. Purple membrane induced alignment of biological macromolecules in the magnetic field. *J. Am. Chem. Soc.* 121:2047–2055.

Stigter, D. 1982a. Coil expansion in polyelectrolyte solutions. *Macromolecules.* 15:635–641.

Stigter, D. 1982b. Mobility of water near charged interfaces. *Adv. Coll. Interf. Sci.* 16:253–265.

Syvitski, R. T., and E. E. Burnell. 1997. Dipole-induced ordering in nematic liquid crystals—fact or fiction? *Chem. Phys. Lett.* 281:199–206.

Syvitski, R. T., and E. E. Burnell. 2000. Dipole-induced ordering in nematic liquid crystals. II. The elusive Holy Grail. *J. Chem. Phys.* 113:3452–3465.

Terzis, A. F., C. D. Poon, E. T. Samulski, Z. Luz, R. Poupko, H. Zimmermann, K. Muller, H. Toriumi, and D. J. Photinos. 1996. Shape-dominated ordering in nematic solvents. A deuterium NMR study of cycloalkane solutes. *J. Am. Chem. Soc.* 118:2226–2234.

Tjandra, N., and A. Bax. 1997. Direct measurement of distances and angles in biomolecules by NMR in a dilute liquid crystalline medium. *Science.* 278:1111–1114.

Tjandra, N., J. G. Omichinski, A. M. Gronenborn, G. M. Clore, and A. Bax. 1997. Use of dipolar H1–N15 and H1–C13 couplings in the structure determination of magnetically oriented macromolecules in solution. *Nat. Struct. Biol.* 4:732–738.

Tjandra, N., S. Tate, A. Ono, M. Kainosho, and A. Bax. 2000. The NMR structure of a DNA dodecamer in an aqueous dilute liquid crystalline phase. *J. Am. Chem. Soc.* 122:6190–6200.

Tolman, J. R. 2002. A novel approach to the retrieval of structural and dynamic information from residual dipolar couplings using several

oriented media in biomolecular NMR spectroscopy. *J. Am. Chem. Soc.* 124:12020–12030.

Tolman, J. R., J. M. Flanagan, M. A. Kennedy, and J. H. Prestegard. 1995. Nuclear magnetic dipole interactions in field-oriented proteins: information for structure determination in solution. *Proc. Natl. Acad. Sci. USA.* 92:9279–9283.

Valafar, H., and J. H. Prestegard. 2003. Rapid classification of a protein fold family using a statistical analysis of dipolar couplings. *Bioinformatics.* 19:1549–1555.

Vroege, G. J., and H. N. W. Lekkerkerker. 1992. Phase transitions in lyotropic colloidal and polymer liquid crystals. *Rep. Prog. Phys.* 55:1241–1309.

Warren, J. J., and P. B. Moore. 2001. Application of dipolar coupling data to the refinement of the solution structure of the Sarcin-Ricin loop RNA. *J. Biomol. NMR.* 20:311–323.

Warshel, A., and J. Aqvist. 1991. Electrostatic energy and macromolecular function. *Annu. Rev. Biophys. Biophys. Chem.* 20:267–298.

Zimmermann, K., H. Hagedorn, C. C. Heuck, M. Hinrichsen, and H. Ludwig. 1986. The ionic properties of the filamentous bacteriophages Pf1 and fd. *J. Biol. Chem.* 261:1653–1655.

Zweckstetter, M., and A. Bax. 2000. Prediction of sterically induced alignment in a dilute liquid crystalline phase: aid to protein structure determination by NMR. *J. Am. Chem. Soc.* 122:3791–3792.

Zweckstetter, M., and A. Bax. 2001. Characterization of molecular alignment in aqueous suspensions of Pf1 bacteriophage. *J. Biomol. NMR.* 20:365–377.

Zweckstetter, M., and A. Bax. 2002. Evaluation of uncertainty in alignment tensors obtained from dipolar couplings. *J. Biomol. NMR.* 23:127–137.